Int J Adv Manuf Technol (2015) 76:2209–2215
DOI 10.1007/s00170-014-6437-8

ORIGINAL ARTICLE

Effect of copper addition on the properties of electroless Ni-Cu-P coating on heat transfer surface

Y. H. Cheng · S. S. Chen · T. C. Jen · Z. C. Zhu · Y. X. Peng

Received: 25 January 2014 / Accepted: 25 September 2014 / Published online: 10 October 2014

Abstract The effect of the copper content on properties of electroless Ni-Cu-P coating on heat exchanger surface was investigated, such as adhesion strength and surface characteristic, and anti-fouling property, which were considered to mitigate the accumulation of mineral fouling in the heat exchangers. The electroless ternary Ni-Cu-P coatings with different copper content were prepared on mild steel (1015) substrate surfaces by adjusting process parameters. Surface morphologies of coating and adhesion strength were investigated by using scanning electron microscopy (SEM) and MFT-4000 multifunctional material surface performance instrument, respectively. The results showed that the adhesion strength was improved with the addition of copper in the coating. With the increase of copper content, the deposition rate of ternary Ni-Cu-P coatings was increased, and the boundary of nodular became obvious. Moreover, the surface free energy of ternary Ni-Cu-P coatings was increased with the increase of copper content in the coatings and then decreased when enhancing the copper content further. The further fouling experiments indicated that all the ternary Ni-Cu-P coating surfaces with different copper content inhibited the adhesion of fouling compared with the stainless steel surface. The adhesion weight of fouling was approximately in proportion with the copper addition of ternary Ni-Cu-P coatings, but not the value of surface free energy. The work provides evidence that both adhesion strength and anti-fouling ability should be combined to use when applying surface modification in the field of heat exchanger.

Y. H. Cheng (✉) · S. S. Chen · Z. C. Zhu · Y. X. Peng
School of Mechanical and Electrical Engineering, China University of Mining and Technology, Xuzhou, People's Republic of China
e-mail: chyh1007@gmail.com

T. C. Jen
School of Engineering, University of Alaska, Fairbanks, AK, USA

Keywords Ternary Ni-Cu-P coating · Adhesion strength · Surface free energy · Anti-fouling · Heat exchanger

1 Introduction

Fouling on heat exchanger surfaces not only is low in thermal conductivity but also reduces the overall heat transfer efficiency of equipment significantly [1]. It was reported that more than 90 % of heat exchangers are puzzled by fouling which degraded seriously the operation of heat exchangers and caused 0.25 % GDP loss in developed countries [2, 3]. This problem could be especially severe in the developing country such as China, due to their lag heat exchangers and low heat transfer efficiency. Therefore, it was essential to study the fouling problem of heat exchanger.

Presently, fouling inhibitors were widely used in industry in order to reduce the adhesion of fouling [4]. However, for one thing, the fouling inhibitors not only cost too much and are used inconveniently but also are prohibited in some conditions (such as drinking water and bathing water) due to their undesired product contamination or adverse environmental effects [5]. For another, the mechanism of fouling inhibitors is not yet fully understood and hence could not be fundamentally solved the problem that fouling attaching on the surface of heat transfer. In recent years, some scholars have developed some varieties of anti-fouling methods in order to reduce the formation of fouling on heat transfer surfaces. The induction period of fouling was extended through changing the surface condition of heat transfer surface, thus resulted in excellent results in inhibiting fouling formation [6].

Kim et al. reported that the heat transfer surface with organic coatings reduces fouling adhering rate. However, the heat transfer capability was degraded [7]. Müller-Steinhagen and Zhao Q. fabricated diamond-like carbon (DLC)-modified surface and inhibited the adhesion of fouling [8, 9]. Ma

investigated the anti-fouling coating by means of dynamic hybrid ion implantation and mixed magnetron sputtering and obviously reduced fouling adhering rate [10]. Liu fabricated nanometer TiO_2 film using liquid phase deposition and restrained the adhesion of $CaCO_3$ fouling [11]. However, these methods, such as "DLC," "ion implantation technology," and "TiO_2 thin film," all have the common characteristics of high cost and need further research before being used widely in the heat exchanger surfaces. In our previous investigations [12], we have reported that Ni-P coatings on the heat transfer surface as a modification surface could gain excellent anti-fouling and heat transfer results. However, the adhesion strength of Ni-P coatings was relatively low and was not suitable for some particular applications in the field of heat exchangers [13–15]. For these reasons, the ternary Ni-Cu-P coatings are investigated in order to improve the reliability of using ternary Ni-Cu-P coating and inhibit the adhesion of mineral fouling in the heat exchanger surface.

2 Experimental methods and materials

2.1 Cases preparation

Mild steels (1015) with a size of 15 mm×15 mm×6 mm are employed as substrates for electroless Ni-Cu-P coatings. Cases were ground using 400; 800; 1,000; and 1,200 SiC waterproof papers and then degreased with a bath of alkaline solution including, respectively, NaOH 20~30 g/l, Na_2CO_3 20~25 g/l, Na_3PO_4 35~40 g/l, and OP-10 4~6 g/l at 80 °C for 15 min. After that, the cases were pickled with a 10 vol% H_2SO_4 solution for 10 s and then activated with a 20 vol% H_2SO_4 solution for 20 s. In between all steps, cases were rinsed with deionized water. Subsequently, Ni-Cu-P coating was electroless deposited on pretreated substrate surface for 2 h at solution temperature of 85 °C and pH value of 9 (adjusted by NaOH solution). All the solutions in the experiment were prepared with chemicals of analytical grade and deionized water. The basic electrolyte was composed of $NiSO_4 \cdot 6H_2O$ (25 g/l), $NaH_2PO_2 \cdot H_2O$ (30 g/l), $C_6H_5Na_3O_7 \cdot 2H_2O$ (40 g/l), and NH_4AC (45 g/l). Meanwhile, the concentrations of copper sulfate in the electroless solutions were 0.2 g/l (case 1), 0.4 g/l (case 2), 0.6 g/l (case 3), and 0.8 g/l (case 4), respectively. Nickel sulfate and sodium hypophosphite are used as sources of nickel and phosphorus, respectively. Ammonium acetate and sodium citrate are applied as complexing agents.

2.2 Surface morphology and adhesion strength test

Surface morphology was observed by an X-3000N-type scanning electron microscopy (SEM) with energy spectrum analysis function. The microstructure characteristics and energy spectrum analysis were carried out with 20.00 keV accelerating voltage. The deposition rate of coatings was measured by MFT-4000 multifunctional material surface performance instrument. The phase structure of the Ni-Cu-P coating is displayed by X-ray diffractometer with Cu Kα radiation. The scanning rate and scanning step are fixed at 4 °C/min and 0.02°, respectively. The adhesion strength of coatings was investigated by using MFT-4000 multifunctional material surface performance instrument (diamond pressure head with 120 cone angle and 0.2-mm tip radius), and the scratch trace was observed by an X-3000N-type scanning electron microscope [16, 17]. The applied load was altered from 0 to 100 N at a constant rate with a sliding speed of 5 mm/min, and the scratch length was 10 mm. The coating thicknesses of cases were managed to control in 12–16 μm by adjusting the deposited time. The measured cases were ultrasonically rinsed in acetone, ethanol, and deionized water in sequence for 2 min before taking the adhesion strength measurement.

2.3 Surface free energy and anti-fouling experiment

Surface free energy is measured at 25 °C. The measured cases are ultrasonically cleaned in acetone, ethanol, and deionized water in sequence for 5 min before surface free energy measurement. The DSA-100 instrument, which is designed and made in German KRÜSS company, is used for testing the surface free energy. A schematic diagram of the fouling experimental rig is given in Fig. 1. The experimental rig consists mainly of six parts, an upper tank, a lower tank with heater, a pump, a temperature control system, an overflow system, and a test system. The total experimental rig is made of stainless steel in order to avoid the influence from corrosive produce. The temperature control system and valve were used to adjust the test temperature and flow velocity. The fouling adhesion experiments are carried out in a supersaturated $CaCl_2$ and $NaHCO_3$ solution at the atmospheric pressure. The cases are placed vertically in the test section, and some crystalline fouling will be adhered on the surface of these testing cases with the lapse of time. For a comparison, the uncoated stainless steel case which is commonly used in heat transfer surface is also suffered the fouling adhering experiment. The fouling weight on the surface of cases is measured in an electronic analytical balance with the accuracy of 10^{-4} g every 4 h after blowing dry. In order to avoid the influence of smooth finish, all the uncoated cases are mechanically grinded and polished before electroless plating experiments. Three group cases were measured, and the average fouling weight on the cases was the fouling adhesion rate.

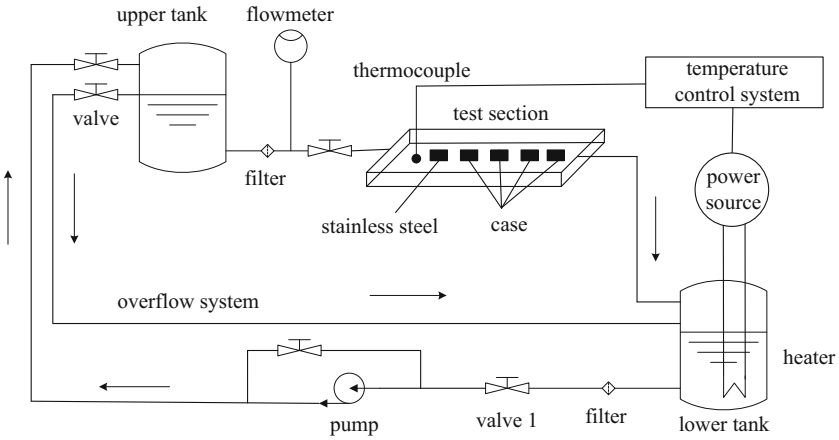

Fig. 1 Schematic diagram of the fouling experimental rig

3 The experimental results and discussion

3.1 Surface morphology and deposition rate

Figure 2 shows the surface morphology of the ternary Ni-Cu-P of cases, which were deposited for 2 h. It is obvious that all the cases exhibit a typical coarse nodular structure. The nodular becomes obvious with the increasing of copper sulfate in the solution, and the nodular could be further divided into finer grains. This result indicates that the amount of copper sulfate in bath has an important effect on the surface morphology. The possible reason is that the amount of copper sulfate affects the plating rate. To verify this conjecture, the thickness of all cases after electroless plating for 2 h was measured, and the results are shown in Fig. 3. As seen from Fig. 3, the deposition rate was almost linearly grown with the increasing of copper sulfate concentration in

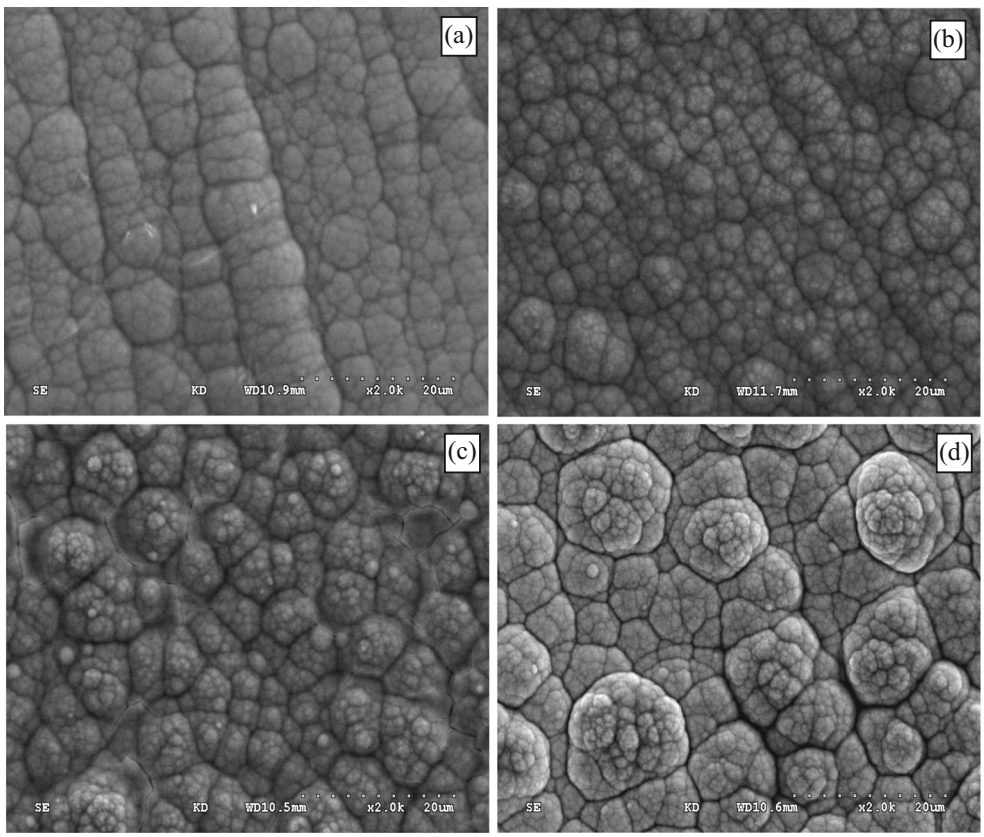

Fig. 2 SEM micrographs of ternary Ni-Cu-P coatings: **a** case 1, **b** case 2, **c** case 3, and **d** case 4

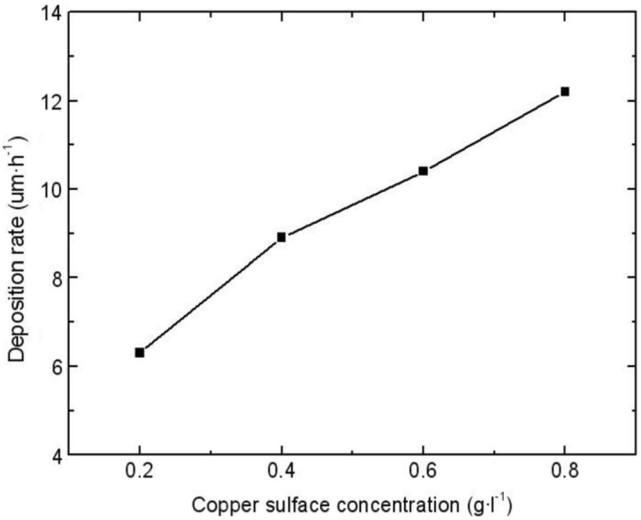

Fig. 3 Effect of copper sulfate concentration on deposition rate

bath. This result indicates that the deposition rate was altered due to the copper sulfate concentration, thus affected the surface morphology.

By further analyzing composition in every case through EDS, it could be found that the copper in the coatings was becoming increased with the increasing of copper sulfate concentration, as showed in Fig. 4. That is to say, the content of copper increased from 2.97 to 13.78 wt% when increasing the copper sulfate concentration from 0.2 to 0.8 g/l. Because it is easy to displace Cu^{+} than the Ni^{+}, the deposition rate becomes increased with the increase of copper ion in the solution. Therefore, the content of copper is increased rapidly when enlarging the concentration of Cu^{2+} in the bath.

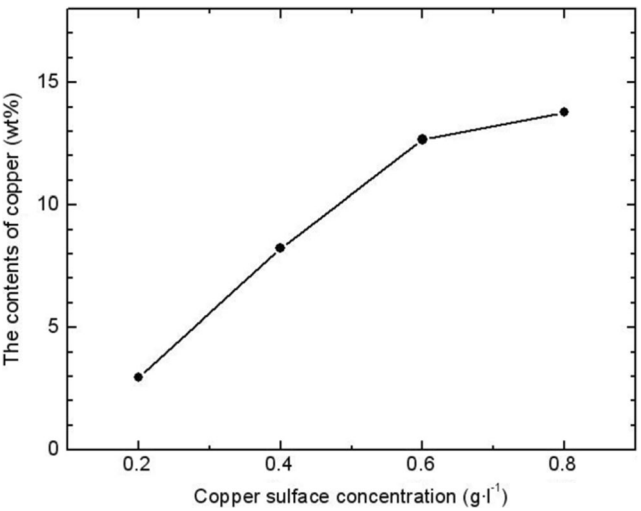

Fig. 4 Content of copper of cases 1, 2, 3, and 4 coatings

3.2 Adhesion strength and X-ray diffraction results

The adhesion strength between coating and substrate is one of the most important performance parameters and was expressed by critical loads [18]. During scratching, the monitored frictional force is used to determine the critical load. The normal load corresponding to the abrupt variation in frictional force due to fracture and/or spallation of coatings is termed as critical load. Following this principle, the normal load of 38 N appeared in Fig. 5 was determined as the adhesion strength value.

Figure 6 indicates the adhesion strength of the coating as a function of case numbers. Combining with the scratch morphology in Fig. 7, it could be clearly seen that the coating happened to strip at the time of critical load. Furthermore, the adhesion strength of coatings goes up gradually with the increasing of copper in the coating and reaches a maximum value at 53 N. This could be attributed to the fact that the coatings were formed on the substrate surface by means of the autocatalytic deposition of copper and nickel ion in the presence of a reducing agent (hypophosphite). The more copper appeared in the interface between substrate and coating and increased the bonding strength which improved the adhesion strength in the process of deposition.

The X-ray diffraction patterns of cases which have been obtained in different processes are shown in Fig. 8. The grain size of the coatings can be calculated approximately by the following Scherrer equation:

$$d = 0.89 \cdot \left(\lambda \Big/ \beta\right) \cdot \cos\theta, \tag{1}$$

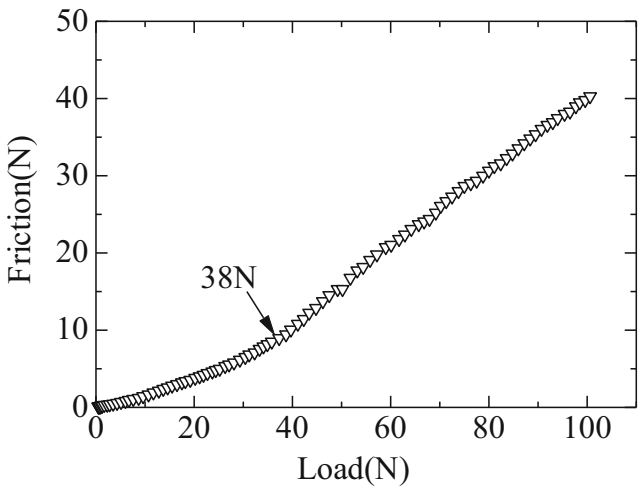

Fig. 5 Friction plot during the scratching test with progressive load (case 1)

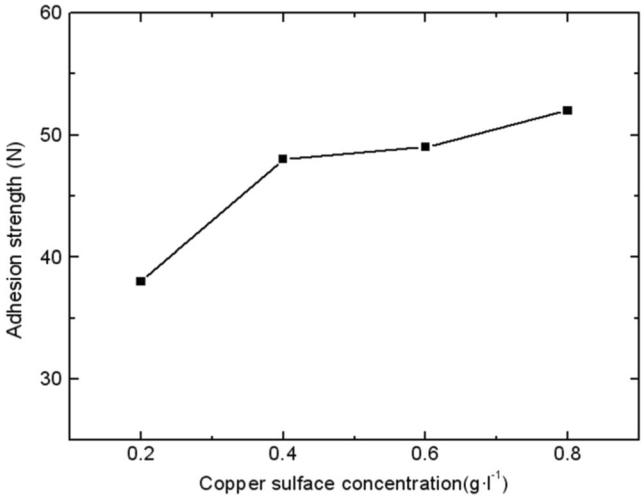

Fig. 6 The adhesion strength variation of cases 1, 2, 3, and 4 coatings

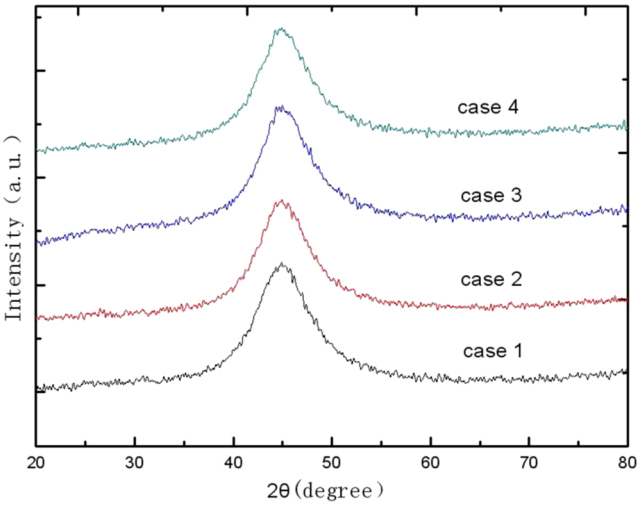

Fig. 8 XRD patterns of cases 1, 2, 3, and 4

where λ is the radiation wavelength, β is the half-maximum width, and θ is the diffraction angle of the main peak.

The corresponding peak position, full width at half maximum, and grain size are given in Table 1. It is obvious from Fig. 8 and Table 1 that all the coatings had only a single broad peak at about 44.8° (2θ) and the grain size of the coatings for cases 1, 2, 3, and 4 is about 2.169, 1.954, 1.835, and 1.685 nm, respectively. A marginal increase in grain size has been observed with the increase of copper in the Ni-Cu-P coatings. And, the grain size of Ni-Cu-P coatings became finer than the Ni-P coatings according to the literature reports on electroless Ni-P coatings [19]. This has further confirmed the finer grain size result caused by copper observed in the morphology of the cases, which are shown in Fig. 2.

3.3 Surface free energy

There are a lot of controversial research results about fouling deposition rate and surface free energy [20]. Figure 9 illustrates the contact angle and surface free energy of pure water on the corresponding Ni-Cu-P coating surfaces, which was measured at ambient temperature and atmospheric pressure. From this figure, it can be seen that all the Ni-Cu-P coatings, whose contact angle values are more than 90°, belong to the surfaces with low surface free energy. Meanwhile, it can also be seen that within the range of concentration of copper sulfate from 0.2 to 0.8 g/l, the surface free energy of the Ni-Cu-P coatings showed an increase trend and reached a maximum value at approximately 26.56 MJ/m^2. However, for higher copper sulfate concentrations, a slight reduction was observed.

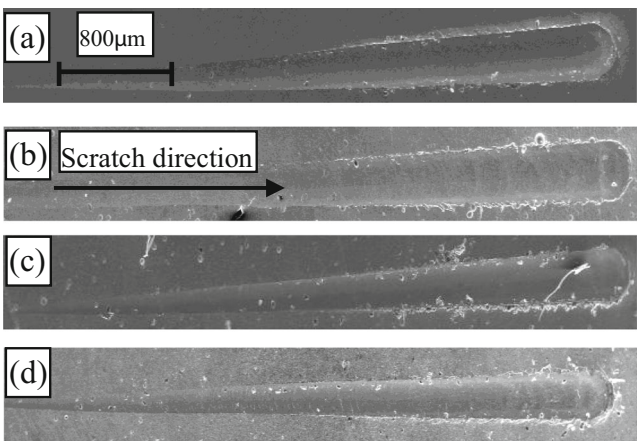

Fig. 7 Micrographs of the scratch channels for Ni-Cu-P coating: **a** case 1, **b** case 2, **c** case 3, and **d** case 4

3.4 Anti-fouling properties of coatings

Figure 10 shows the relation between the crystallization fouling weight per unit area and the time elapsing for the Ni-Cu-P coatings and uncoated stainless steel which are carried out in the fouling adhering experiments in the supersaturated $CaCl_2$ and $NaHCO_3$ solution container for 20 h. It is evident that the amount of the crystallization fouling on the Ni-Cu-P coating surfaces has significantly decreased in comparison with that on the uncoated stainless steel case. It can also be seen that the fouling on the coating surfaces of cases 1, 2, 3, and 4 differs

Table 1 Peak position, full width at half maximum, and grain size for the Ni-Cu-P coatings

Case number	Peak position	FWHM	Grain size (nm)
1	44.874	3.902	2.169
2	45.008	4.354	1.954
3	44.996	4.636	1.835
4	44.874	5.046	1.685

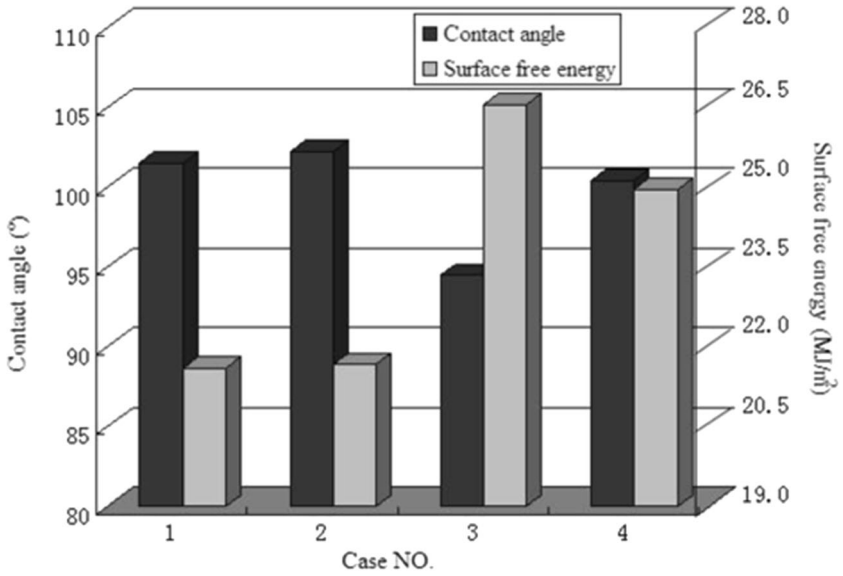

Fig. 9 Surface free energy and contact angle of cases 1, 2, 3, and 4

from each other. More specifically, there appeared to be the most fouling on the coating surface of the case 4. Combining with the results of composition and surface free energy obtained in "Surface morphology and deposition rate" and "Surface free energy" sections, it can be speculated that the increase trend of fouling adhesion is consistent with the increase of the copper addition in ternary Ni-Cu-P coatings, but not the value of surface free energy. This result is same as that of Zhao and Liu [21], and in that paper, the authors also reported different results that minimal adhesion of $CaSO_4$ corresponded to a range of surface free energy. That is to say, the adhesion amount of fouling is not always decreased with the decreasing of surface free energy. Therefore, the surface free energy should not be looked as the criterion that assesses anti-fouling properties of the heat transfer surface although the Ni-Cu-P coatings with low surface free energy exhibit excellent anti-fouling ability than stainless steel with higher surface free energy.

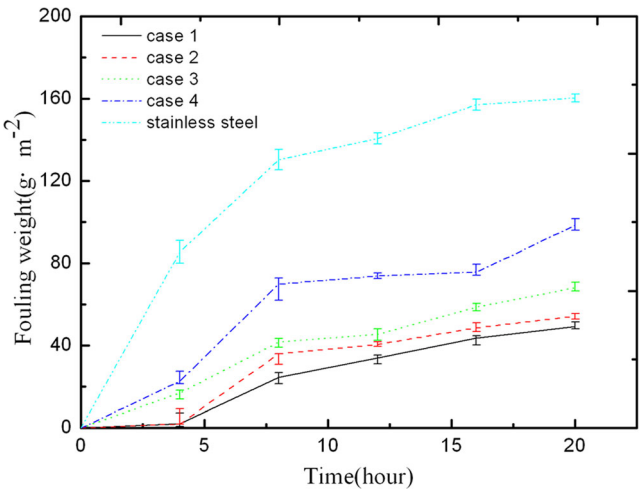

Fig 10 Fouling adhering weight versus time on Ni-Cu-P coating surfaces

4 Conclusions

Ternary Ni-Cu-P coatings were prepared by means of electroless plating. The effect of the copper content on surface morphology, adhesion strength of electroless Ni-Cu-P coatings, surface free energy, and anti-fouling properties was investigated. The conclusions are as follows:

1. Ternary Ni-Cu-P coatings indicate a typical nodular feature. The boundary of nodular becomes obvious with the increasing of copper sulfate in the solution because of the increase of deposition rate. And, the copper in all coatings was becoming increased with the increasing of copper sulfate in the bath.
2. The adhesion strength of ternary Ni-Cu-P coatings goes up gradually with the increasing of copper composition in the coatings due to the stronger interface bonding between substrate and coating.
3. The surface free energy of all the ternary Ni-Cu-P coatings becomes slightly larger when the concentrations of copper sulfate become increased. However, when the concentrations of copper sulfate become higher further, the surface free energy becomes slightly decreased. The ternary Ni-Cu-P coatings manifest excellent anti-fouling properties. The distinction should be considered between higher surface free energy and lower surface free energy when we assess the anti-fouling properties of the heat transfer surface.

Acknowledgments This work is supported by the National Basic Research Program of China (2013CB228305) and the Fundamental Research Funds for the Central Universities (2012QNA26) and a project funded by the Priority Academic Program Development of Jiangsu Higher Education Institutions.

References

1. Al-Janabi A, Malayeri MR, Müller-Steinhagen H (2010) Experimental fouling investigation with electroless Ni-P coatings. Int J of Therm Sci 49:1063–1071
2. Kazi SN, Duffy GG, Chen XD (2012) Fouling and fouling mitigation on heated metal surfaces. Desalination 288:126–134
3. Bornhorst A, Müller-Steinhagen H, Zhao Q (1999) Reduction of scale formation by ion-implantation and magnetron sputtering on heat transfer surfaces. Heat Transfer Eng 20:6–14
4. Yang QF, Gu AZ, Ding J (2002) Calcium carbonate fouling behavior and morphology. J Chem Ind Eng 53:924–930
5. Yang SR, Sun LF, Xu ZM (2004) Development and prospect of research on heat exchanger fouling. Chem Ind Eng Prog 23:1091–1098
6. Cheng YH, Chen HY, Zhu ZC, Jen TC, Peng YX (2014) Experimental study on the anti-fouling effects of Ni-Cu-P-PTFE deposit surface of heat exchangers. Appl Therm Eng 68:20–25
7. Lee J, Kim TJ, Kim MH (2005) Experimental study on the heat and mass of teflon-coated tubes for the latent heat recovery. Heat Transfer Eng 26:28–37
8. Zhao Q, Wang X (2005) Heat transfer surfaces coated with fluorinated diamond-like carbon films to minimize scale formation. Surf Coat Technol 192:77–80
9. Rosmaninho R, Santos O, Nylander T (2007) Modified stainless steel surfaces targeted to reduce fouling—evaluation of fouling by milk components. J Food Eng 80:1176–1187
10. Ren XG, Li TF, Zhao Q (2006) Effect of surface treatment on flow boiling heat transfer coefficient in CaSO4 containing water. Chin J Chem Eng 14:122–126
11. Wang LL, Liu MY (2009), Antifouling and anticorrosion properties on surfaces of TiO_2 nanometer films coated with liquid phase deposition, Proc. of Int. Conference on Heat Exchanger Fouling and Cleaning VIII-2009: 281–288
12. Cheng YH, Zou Y, Cheng L, Liu W (2009) Effect of the microstructure on the anti-fouling property of the electroless Ni-P coating. Mater Lett 62:4283–4285
13. Nemeth S (2008) Modelling of the scratch resistance of particle filled sol-gel coatings on aluminium. Thin Solid Films 516:5355–5359
14. Zhang WX, Huang N, He JG et al (2007) Electroless deposition of Ni-W-P coating on AZ91D magnesium alloy. Appl Surf Sci 253: 5116–5121
15. Boentoro W, Pflug A, Szyszka B (2009) Scratch resistance analysis of coatings on glass and polycarbonate. Thin Solid Films 517: 3121–3125
16. Krump H, Simor M, Hudec I, Jasso M, Luyt AS (2005) Adhesion strength study between plasma treated polyester fibres and a rubber matrix. Appl Surf Sci 240:268–274
17. Song WL, Deng JX, Yan P, Wu Z, Zhang H, Zhao J, Ai X (2011) Influence of negative bias voltage on the mechanical and tribological properties of MoS2/Zr composite films. J Wuhan Univ Technol Mater Sci Ed 126:412–416
18. Huang RX, Qi ZB, Sun P, Wang ZC, Wu CH (2011) Influence of substrate roughness on structure and mechanical property of TiAlN coating fabricated by cathodic arc evaporation. Phys Procedia 18: 160–167
19. Cheng YH, Zou Y, Cheng L, Liu W (2009) Effect of the microstructure on the properties of Ni–P deposits on heat transfer surface. Surf Coat Technol 203:1559–1564
20. Connell CO, Sherlock R, Ball MD et al (2009) Investigation of the hydrophobic recovery of various polymeric biomaterials after 172 nm UV treatment using contact angle surface free energy and XPS measurements. Appl Surf Sci 255: 4405–4413
21. Zhao Q, Liu Y (2006) Modification of stainless steel surfaces by electroless Ni-P and small amount of PTFE to minimize bacterial adhesion. J Food Eng 72:266–272